

Artificial Intelligence for Estimating Multiple Irradiation Conditions from Temperature Distribution

Miki Nakaone¹, Tomomasa Ohkubo^{*1}, Yuki Ueno¹, Ken Goto², and Yutaka Kagawa³

¹Graduate School of Engineering, Tokyo University of Technology

²Institute of Space and Astronautical Science, Japan Aerospace Exploration Agency

³Katayanagi Institute, Tokyo University of Technology

*Corresponding author's e-mail: ookubotmms@stf.teu.ac.jp

An accelerated heating test method named Selective Laser Thermoregulation (SLT) is capable of dynamically controlling heat input by scanning a laser. Therefore, the irradiation conditions of the SLT system are highly flexible. The development of AI, which predicts the irradiation conditions that can reproduce the required temperature distribution, is required to determine the irradiation conditions automatically. In this paper, we report the development of AI that suggests irradiation conditions that can reproduce the required temperature distribution when irradiating a laser at a fixed point. The AI well predicted the irradiation coordinates, but it predicted the laser power, the beam radius, and the irradiation time different from the original values. However, the temperature distributions calculated using the irradiation conditions predicted by AI and the required temperature distributions were similar. We evaluated the similarity of the temperature distribution; 94.6% of data of MAPE are less than 5%.

DOI: 10.2961/jlmn.2022.03.3001

Keywords: selective laser thermoregulation (SLT) system, laser heating, AI, fully connected neural network, machine learning

1. Introduction

Aircraft is essential for us in an increasingly globalized world. SiC/SiC ceramic composites (CMCs) are expected to improve the efficiency of aircraft engines. SiC/SiC CMCs are materials that have the properties of higher specific strength and heat resistance than the alloys currently used in aircraft engines [1][2]. However, the mechanical properties of SiC/SiC CMCs in a high-temperature environment are not exactly known. In order to use this material as an aircraft engine, a heating test of it is necessary.

Many studies have measured the physical properties of SiC/SiC CMCs in a high-temperature environment [3]-[6]. An actual aircraft engine is repeatedly heated and cooled over a long time. Therefore, it is necessary to perform accelerated heating tests.

In order to heat the material in a short time, some researchers reported heating test methods that use a high-power laser. Appleby reported a heating test method using a CO₂ laser in 2015 [7]. However, it is difficult to perform experiments in high humidity and high-temperature environment that simulates the actual environment of an aircraft engine because water vapor absorbs a CO₂ laser. Whitlow reported the laser heating test systems using a fiber laser in 2019 [8]. The fiber laser has a wavelength of 1.07 μm, which is not easily absorbed by water vapor compared with the wavelength of the CO₂ laser [9]. However, static optics shaped the beam into a test piece's shape before irradiation in this system. Therefore, this method makes it difficult to compensate the heat input dynamically to achieve an optimal temperature distribution.

We developed an accelerated heating test method named "Selective Laser Thermoregulation (SLT)" [10].

The SLT system can dynamically control heat input by scanning the laser whose absorptivity of water vapor is low. The previous study used a fiber laser and a galvano mirror system. However, to realize the required temperature distribution, we must adjust the multiple irradiation conditions, such as irradiation coordinates, laser power, beam radius, and irradiation time. Determining irradiation conditions to reproduce the required temperature distribution accurately is time-consuming because the irradiation conditions are highly flexible, and many patterns are possible.

Therefore, we developed AI to estimate laser irradiation conditions that reproduce the required temperature distribution. In previous research, we developed AI that estimates laser power, which is the most fundamental parameter [11]. However, the previous study did not estimate or evaluate the temperature distribution. In this study, we increased the number of conditions predicted by AI to five. Moreover, we evaluated the temperature distributions, which were calculated using the irradiation conditions predicted by AI.

The final goal of this study is to develop AI that estimates the irradiation conditions to reproduce the required temperature distribution using a scanning laser with complex paths. However, the more complex the laser scanning conditions, the more complicated the development of AI becomes. Since developing complex AI in the current step is challenging, we chose a simple system with fixed-point irradiation as our target. In other words, this study aims to achieve AI that estimates the irradiation conditions from the temperature distribution when the laser is irradiated at a single point without scanning the laser.

Firstly, we generated temperature distribution by numerical simulation for use in the learning and evaluation of

our AI. Although we can get the temperature distribution by experiment, a large amount of data is required for training AI. Therefore, we used the temperature distribution calculated by numerical simulation in this study because they are relatively easy to collect. However, AI using a dataset from numerical simulation and AI using experimental data may produce different results. Therefore, this study aims to develop AI that can learn about the causal relationship between laser irradiation conditions and temperature distribution. If such a framework is created, we consider that it will be possible to have AI that predicts irradiation conditions for experiments by changing the learning data from numerical calculations to experiments in the future. Secondly, we evaluated the irradiation conditions predicted by AI. Finally, we assessed whether the irradiation conditions predicted by AI achieve the purpose of this study, which is to reproduce the required temperature distribution.

2. Generating a dataset by numerical simulation

We generated a dataset of the relationship between the laser irradiation conditions and the temperature distribution by numerical simulation for teaching and evaluating our AI. The parameters used in this study are shown in Table 1. We generated a total of 16807 temperature distributions by changing the irradiation conditions such as irradiation coordinates of x and y , laser power, beam radius, and irradiation time. We divided the dataset randomly into training data and test data. 80% of the data was used as training data, and the remaining 20% as test data.

We generated the temperature distribution by numerical simulation. An analytical solution can create the temperature distribution realized by single-point irradiation, which is used in this study. However, the temperature distribution realized by the scanning laser with a complex path that will be used in future studies cannot be generated by an analytical solution. Therefore, we used our numerical simulation code developed in the previous study [11]. The numerical simulation code solved the heat balance of the input laser power, thermal conduction, heat transfer to the air, and radiation using the finite difference method in two dimensions.

Fig. 1 is the result of the numerical simulation whose irradiation coordinates are $x = 0.0$ mm, $y = 0.0$ mm, the laser power is 2000 W, the beam radius is 8 mm, and the irradiation time is 0.8 s. The shape of the test piece was 41 mm \times 41 mm \times 3 mm (thickness). The origin of the coordinate system is the center of the test piece. The laser was irradiated at a single point.

Table 1 Details of the irradiation conditions for the numerical simulations

	Range	Step	Patterns
x coordinate [mm]	-12 to 12	4	7
y coordinate [mm]	-12 to 12	4	7
Laser power [W]	400 to 400	600	7
Beam radius [mm]	2 to 8	1	7
Irradiation time [s]	0.2 to 0.8	0.1	7

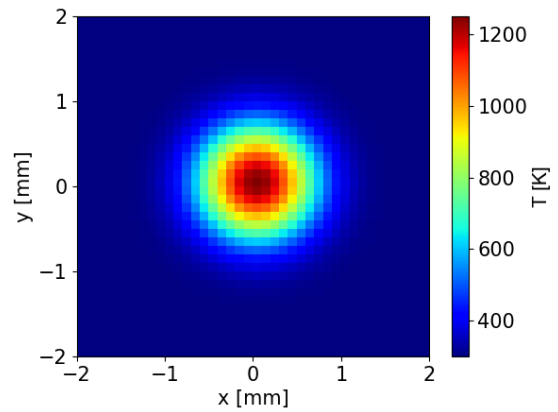


Fig. 1 Example of visualization of temperature distribution generated by numerical calculation

We developed five types of fully connected neural networks (FCNNs): FCNN to predict an irradiation coordinate x , an irradiation coordinate y , a laser power, a beam radius, and an irradiation time. The input of each FCNN is the temperature distribution, and the output is a predicted irradiation condition. The prediction target differs for each FCNN, but all FCNNs have the same configuration. The neural network configuration of this study is shown in Fig. 2. Firstly, the temperature distribution as the input to the FCNNs is the 2D temperature distribution with 41 rows and 41 columns. We flattened the 2D data to a 1D vector of 1681 elements to use fully connected layers. Secondly, there are three fully connected layers with nodes of 500, 100, and 30. Finally, the FCNN outputs predicted each irradiation condition.

The activation function of each node is the ReLU function [12] except the last, and the last is the identity function. The loss function is the mean square error. The optimizer is the root mean square propagation.

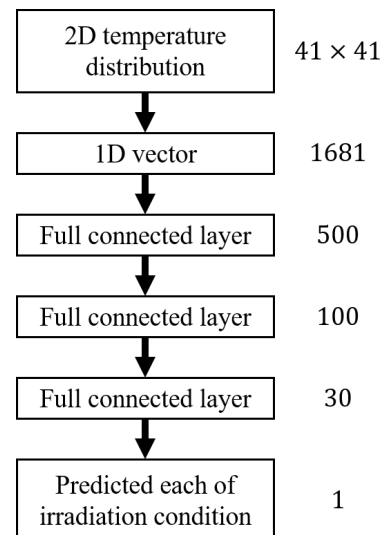


Fig. 2 Neural network configuration for estimating. The numbers on the right side are the node size.

3. Evaluation

To evaluate the FCNNs, we made the FCNNs predict the irradiation conditions from the temperature distribution using test data that was not used in the learning steps. The temperature distribution test data are described as “the original temperature distribution”, and the irradiation conditions used for the temperature distribution are described as “the original irradiation conditions” in the following descriptions.

We made two types of evaluations for the FCNNs. We evaluated whether the FCNNs can correctly predict the irradiation conditions. Furthermore, we evaluated the temperature distribution calculated from the irradiation conditions predicted by the FCNNs.

3.1. Evaluation of the irradiation conditions

Fig. 3 shows the relationship between the original irradiation conditions and the irradiation conditions predicted by the FCNNs. The points are the results, and the dashed line indicates the case of the predicted is the same value as the original value.

As shown in Fig. 3 of (a) and (b), almost all points are near the dashed lines. Therefore, the FCNNs could predict the irradiation coordinates close to the original coordinates.

On the other hand, as shown in Fig. 3 of (c), (d), and (e), a lot of the points deviate from the dashed line. Therefore, the FCNNs predict the irradiation conditions of the laser power, the beam radius, and the irradiation time with low accuracy.

3.2. Evaluation of the temperature distribution

We compared the original temperature distribution with the temperature distribution simulated using the irradiation conditions predicted by the FCNNs. The evaluation function of Mean Absolute Percentage Error (MAPE), shown in equation (1), was used for the evaluation.

$$MAPE = \frac{100}{n} \sum_{i=1}^n \left| \frac{\alpha_k - \beta_k}{\beta_k} \right| \quad (1)$$

n , α_k , and β_k are the number of data, the predicted value (calculated temperature of the k -th cell), and the original value (original temperature of the k -th cell), respectively. The smaller MAPE means that the error between the original temperature distribution and the temperature distribution realized using the irradiation conditions predicted by the FCNNs is smaller.

Fig. 4 shows the evaluated result of the temperature distributions. Most data of MAPE were between 1% and 2%. Furthermore, 94.6% of the data of MAPE had less than 5%.

4. Discussion

The temperature distribution changes when the irradiation coordinates, the laser power, the beam radius, and the irradiation time are changed. The position of the maximum temperature depends on the irradiation coordinates. Therefore, the irradiation coordinates could be predicted with high accuracy, as shown in Fig. 3 of (a) and (b), because the position of the maximum temperature is not affected by other irradiation conditions. On the other hand, the maxi-

imum temperature and the high-temperature region depend on some of the laser power, the beam radius, and the irradiation time. For example, energy density [J/m^2] depends on three parameters: laser power, beam radius, and irradiation time. Therefore, as the values of these three parameters vary, the energy density also varies. That is because the effects of these three irradiation conditions on the temperature distribution are similar; these three irradiation conditions are difficult to predict from temperature distribution, as shown in Fig. 3 of (c), (d), and (e).

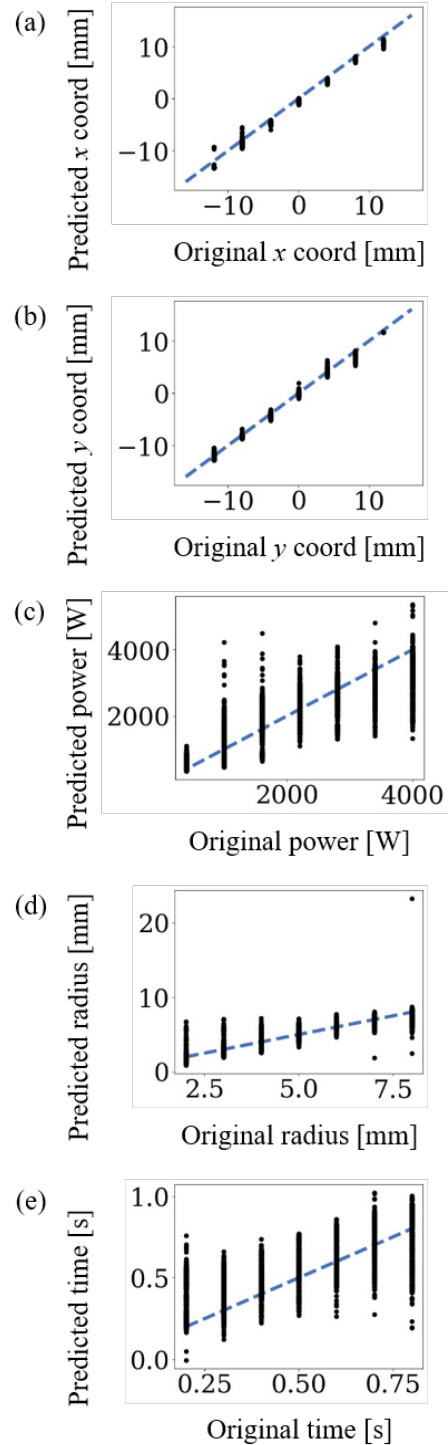


Fig. 3 Relationship between the original value and the predicted values. (a) irradiation coordinate x , (b) irradiation coordinate y , (c) laser power, (d) beam radius, (e) irradiation time

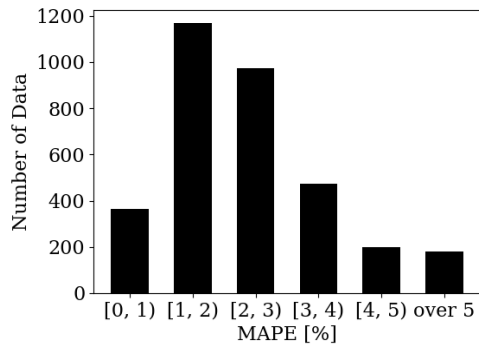


Fig. 4 Number of MAPE data in test data

Although the FCNNs predicted different irradiation conditions from the original irradiation conditions, the MAPE of the predicted temperature distribution is sufficiently small, as shown in Fig. 4. Therefore, it is possible to realize the original temperature distribution using the estimated irradiation parameters by the FCNNs, even if the parameters are different from the original irradiation conditions within the range of the parameters changed in this study.

For example, Fig. 5 shows the original temperature distribution, and Fig. 6 shows the temperature distribution calculated using the irradiation conditions predicted by the FCNNs. There is no significant visible difference between the two temperature distributions. In addition, the MAPE of this prediction was 2.69%. However, the irradiation conditions for Fig. 5 and Fig. 6 are different. Fig. 5 is the calculated result using the laser power of 3400 W, the beam radius of 5.0 mm, and the irradiation time of 0.20 s. On the other hand, Fig. 6 is the calculated result using the laser power of 1690 W, the beam radius of 4.9 mm, and the irradiation time of 0.50 s. There are differences of 1710 W for the laser power, 0.1 mm for the beam radius, and 0.30 s for the irradiation time. Therefore, we clarified that even if the FCNNs did not predict the original irradiation conditions, the required temperature distribution could be reproduced by the irradiation conditions predicted by the FCNNs.

As discussed in this section, the predicted irradiation conditions by the FCNNs appear to be wrong when evaluating only the irradiation conditions, and it is difficult to predict original irradiation conditions such as the laser power, the beam radius, and the irradiation time. However, it is not necessary to predict the original irradiation conditions to reproduce the required temperature distribution. Because there was a sufficiently small MAPE between the original temperature distribution and the temperature distribution calculated using the irradiation conditions predicted by the FCNNs, we confirmed that our purpose of reproducing the required temperature distribution could be achieved by the FCNNs developed in this study.

5. Conclusions

We developed FCNNs for estimating the laser irradiation conditions from temperature distribution.

When our FCNNs were evaluated using the irradiation conditions, it predicted the irradiation coordinates close to the original values. However, the laser power, the beam radius, and the irradiation time of the predicted values deviated from the original values.

On the other hand, we evaluated FCNNs by the temperature distribution and confirmed that 94.6% of the data are predicted with MAPE of less than 5%. We confirmed that the conditions predicted by our FCNNs reproduced the required temperature distribution.

6. Future works

Although we used the temperature distribution calculated by numerical simulation in this study, learning and evaluation using the experimental data is our future work.

Laser power, beam radius, and irradiation time, whose predictions did not match the original values, strongly influence the two-dimensional temperature distribution. However, in this study, we used the most basic neural network of the FCNN without considering that tendency. To overcome this problem, we expect that a convolutional neural network (CNN) used in image processing and classification is better for predicting the irradiation conditions from two-dimensional temperature distribution. Furthermore, if AI estimates the laser irradiation conditions for a scanning laser, we consider that a recurrent neural network usually used for predicting time series data may be more suitable. We will consider these other machine learning methods in future works.

Furthermore, if the material of the target used in the laser heating test changes, the physical properties, such as the absorption rate of the laser, specific heat, and thermal conductivity, also change. When the physical properties change, the temperature distribution that is the input for AI also changes. Although this study does not assume such material changes, we will develop AI that can correctly predict the required laser irradiation conditions from the temperature distribution of different materials in future works.

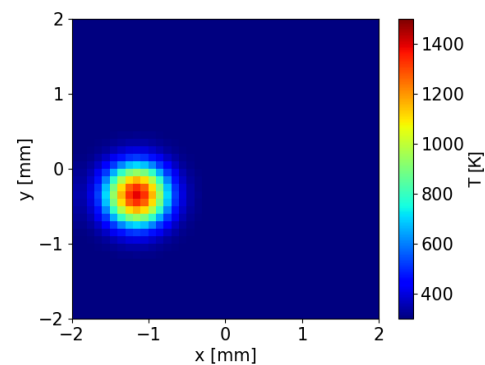


Fig. 5 Example of the original temperature distribution

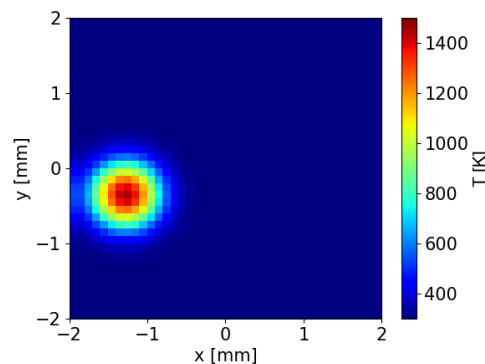


Fig. 6 Example of the temperature distribution predicted by the FCNNs

Acknowledgments and Appendixes

This paper is based on results obtained from a project, JPNP20004, subsidized by the New Energy and Industrial Technology Development Organization (NEDO).

References

- [1] G.S. Corman and K.L. Luthra: "Handbook of Ceramic Composites" ed. by N. P. Bansal, (Publisher, Boston, 2005) p.99.
- [2] M. Roode, J. Price, J. Kimmel, N. Miriyala, D. Leroux, A. Fahme, and K. Smith: *J. Eng. Gas Turbines Power*, 129, (2007) 21.
- [3] R. J. Young, A. B. L. Broadbridge, and C.-L. So: *J. Microscopy*, 196, (1999) 257.
- [4] Y. L. Dong, H. Kakisawa, and Y. Kagawa: *Meas. Sci. Technol.*, 25, (2014) 025002.
- [5] A. Haboub, H. A. Bale, J. R. Nasiatka, B. N. Cox, D.B. Marshall, R. O. Ritchie, and A. A. MacDowell: *Rev. Sci. Instrum.*, 85, (2014) 083702.
- [6] T. Whitlow, E. Jones, and C. Przybyla: *Compos. Struct.*, 158, (2016) 245.
- [7] M.P. Appleby, D. Zhu, and G. Morscher: *Surf. Coat Technol.*, 284, (2015) 318.
- [8] T. Whitlow, J. Pitz, J. Pierce, S. Hawkins, A. Samuel, K. Kollins, G. Jefferson, E. Jones, J. Vernon, and C. Przybyla: *Compos. Struct.*, 210, (2019) 179.
- [9] W. M. Irvine and J. B. Pollack, *Icarus*, 8, (1968) 324.
- [10] H. Koshiji, T. Ohkubo, K. Azato, Y. Kameda, E. Matsunaga, T. Dobashi, N. Shichijo, K. Goto, M. Sato, C. Fujiwara, and Y. Kagawa: *J. Laser Micro Nanoeng.*, 15, (2020) 174.
- [11] M. Nakaone, T. Ohkubo, Y. Ueno, K. Goto, and Y. Kagawa: *J. Laser Micro Nanoeng.*, 16, (2021) 84.
- [12] X. Glorot, A. Bordes, and Y. Bengio: *Proc. 14th International Conference on Artificial Intelligence and Statistics*, (2011) 315.

(Received: May 31, 2022, Accepted: November 4, 2022)